Walking near a Conformal Fixed Point: the 2-d $O(3)$ Model at $\theta \approx \pi$ as a Test Case

P. de Forcrand[a,b] , M. Pepe[c], and U.-J. Wiese[d]
[a] *Institute for Theoretical Physics, ETH Zürich, CH-8093 Zürich, Switzerland*
[b] *CERN, Physics Department, TH Unit, CH-1211 Genève 23, Switzerland*
[c] *INFN, Istituto Nazionale di Fisica Nucleare, Sezione di Milano-Bicocca Edificio U2, Piazza della Scienza 3, 20126 Milano, Italy*
[d] *Albert Einstein Center for Fundamental Physics, Institute for Theoretical Physics, Bern University, Sidlerstrasse 5, CH-3012 Bern, Switzerland*

Slowly walking technicolor models provide a mechanism for electroweak symmetry breaking whose nonperturbative lattice investigation is rather challenging. Here we demonstrate walking near a conformal fixed point considering the 2-d lattice $O(3)$ model at vacuum angle $\theta \approx \pi$. The essential features of walking technicolor models are shared by this toy model and can be accurately investigated by numerical simulations. We show results for the running coupling and the beta-function and we perform a finite size scaling analysis of the massgap close to the conformal point.

The scalar Higgs field that drives spontaneous electroweak symmetry breaking in the Standard Model is considered unnatural as a fundamental degree of freedom because it suffers from the gauge hierarchy problem. Technicolor provides a promising mechanism that stabilizes the electroweak scale against the Planck or GUT scale by introducing a new asymptotically free strongly coupled gauge theory [1]. The chiral condensate of techniquarks then induces electroweak symmetry breaking and replaces the fundamental Higgs field in a natural way, i.e. without fine-tuning. The original technicolor models [2–4] suffer from flavor-changing neutral currents. In addition, electroweak precision tests are strongly affected by the running of the technicolor gauge coupling [5]. In order to avoid these problems, it has been proposed to consider slowly walking technicolor theories [6–8]. In these models the running of the gauge coupling slows down due to the proximity to a conformal fixed point [9]. Besides non-Abelian technicolor gauge fields, these models usually contain many flavors of techniquarks in the fundamental representation or technifermions in higher-dimensional representations of the technicolor gauge group. In order to naturally stabilize the electroweak scale against the Planck scale, these models are still asymptotically free. They are just outside the conformal window of theories that have an infrared conformal and an ultraviolet asymptotically free fixed point. The lower edge of the conformal window corresponds to the merging of two fixed points and thus to a double zero of the β-function [10, 11]. Determining whether a theory is inside or near the conformal window requires nonperturbative investigations, which can be performed from first principles using lattice gauge theory. Lattice theories with different gauge groups and with different fermionic matter content have been studied quite intensively [12–18]. Due to finite-size and finite lattice spacing effects as well as due to difficulties with simulating nearly massless dynamical fermions, investigating whether a theory is inside the conformal window is a difficult task. Determining whether a theory is slowly walking is even more challenging. At present, there is no consensus on which theories are slowly walking.

In this paper, for the first time we unambiguously demonstrate walking near a conformal fixed point in an asymptotically free field theory — the 2-d $O(3)$ model, which shares many features with 4-d non-Abelian gauge theories. In particular, besides being asymptotically free, it has a dynamically generated massgap, instantons, and thus a non-trivial vacuum angle θ. At $\theta = 0$, the Euclidean action of the model is given by

$$S[\vec{e}] = \frac{1}{2g^2} \int d^2x \; \partial_\mu \vec{e} \cdot \partial_\mu \vec{e}. \tag{1}$$

Here $\vec{e}(x)$ is a 3-component unit-vector field and g is the coupling constant. The topological charge,

$$Q[\vec{e}] = \frac{1}{8\pi} \int d^2x \; \varepsilon_{\mu\nu} \vec{e} \cdot (\partial_\mu \vec{e} \times \partial_\nu \vec{e}) \in \Pi_2[S^2] = \mathbb{Z}, \tag{2}$$

contributes an additional term $i\theta Q[\vec{e}]$ to the action. The 2-d $O(3)$ model is integrable at $\theta = 0$ [19–21] as well as at $\theta = \pi$ [22], but not at intermediate values of θ. The massgap at $\theta = 0$ has been determined analytically [23] and is given by $M = \frac{8}{e}\Lambda_{\overline{MS}}$, where e is the base of the natural logarithm and $\Lambda_{\overline{MS}}$ is the scale that is dynamically generated by dimensional transmutation in the modified minimal subtraction scheme. As one varies θ, the massgap is reduced until it finally vanishes at $\theta = \pi$. The conjectured exact S-matrix at $\theta = \pi$ has recently been confirmed by lattice simulations with per mille level accuracy [24]. This study has also demonstrated beyond any reasonable doubt that θ is a relevant parameter that does not get renormalized nonperturbatively. Consequently, each value of θ characterizes a different physical theory, which was further supported by [25].

As one infers from the exact S-matrix [22], at energies far below $\Lambda_{\overline{MS}}$ the 2-d $O(3)$ model at $\theta = \pi$ reduces to

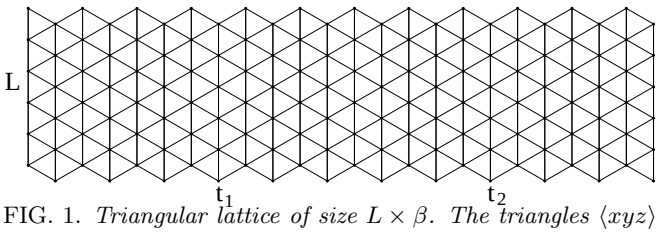

FIG. 1. *Triangular lattice of size $L \times \beta$. The triangles $\langle xyz \rangle$ carry the topological term $i\theta q_{\langle xyz \rangle}$. The correlation function $C(t_1, t_2; \theta)$ is determined between the time-slices at t_1 and t_2.*

the $k = 1$ WZNW model [26–28], a conformal field theory with the Euclidean action

$$S[U] = \frac{1}{2g'^2} \int d^2x \ \mathrm{Tr}[\partial_\mu U^\dagger \partial_\mu U] - 2\pi i k S_{WZNW}[U]. \quad (3)$$

Here $U(x) \in SU(2) = S^3$ and g' is a coupling constant. The Wess-Zumino-Novikov-Witten term is given by

$$S_{WZNW}[U] = \frac{1}{24\pi^2} \int_{H^3} d^2x \ dx_3 \ \varepsilon_{\mu\nu\rho} \mathrm{Tr}[U^\dagger \partial_\mu U U^\dagger \partial_\nu U U^\dagger \partial_\rho U]. \quad (4)$$

Here H^3 is a 3-d hemisphere whose boundary $\partial H^3 = S^2$ is the compactified 2-d space-time. Since $\Pi_2[S^3] = \{0\}$, there are no topological obstructions against extending the 2-d field $U(x)$ on $x \in S^2$ to a 3-d field $U(x, x_3)$ on $(x, x_3) \in H^3$. The WZNW-terms corresponding to two different extensions $U^{(1)}$ and $U^{(2)}$ differ by an integer,

$$S_{WZNW}[U^{(1)}] - S_{WZNW}[U^{(2)}] = \frac{1}{24\pi^2} \int_{S^3} d^2x \ dx_3 \times \varepsilon_{\mu\nu\rho} \mathrm{Tr}[U^\dagger \partial_\mu U U^\dagger \partial_\nu U U^\dagger \partial_\rho U] \in \Pi_3[S^3] = \mathbb{Z}. \quad (5)$$

Here two hemispheres have been combined to form a sphere S^3 with U corresponding to $U^{(1)}$ on one and to $U^{(2)}$ on the other hemisphere. Since $S_{WZNW}[U]$ is thus well-defined only up to an integer, in order to obtain an unambiguous contribution $\exp(2\pi i k S_{WZNW}[U])$ to the functional integral, the level k must be quantized in integer units. Interestingly, the WZNW model has a global $SU(2)_L \times SU(2)_R$ symmetry, $U(x)' = L U(x) R^\dagger$, which extends the $O(3)$ symmetry to $O(4)$. It should be noted that only the low-energy WZNW sector, but not the entire $O(3)$ model at $\theta = \pi$ has the enlarged $O(4)$ symmetry. The scale $\Lambda_{\overline{MS}}$, which results from anomalous scale breaking and dimensional transmutation, still induces explicit symmetry breaking down to $O(3)$. Due to the enlarged $O(4)$ symmetry of the low-energy sector, an $O(3)$ singlet becomes degenerate with the $O(3)$ triplet as $\theta \to \pi$ [29].

Since the WZNW model is a conformal field theory, the 2-d $O(3)$ model at $\theta \approx \pi$ is a natural candidate for a slowly walking asymptotically free theory near a conformal fixed point [25]. Following [30, 31], we define a running coupling constant $\alpha(\theta, L) = g^2(\theta, L) \equiv m(\theta, L)L$ through the massgap $m(\theta, L)$ in a periodic volume of spatial size L. At small L the coupling $\alpha(\theta, L)$ can be computed in perturbation theory. In this limit, it is independent of the vacuum angle θ, which does not affect perturbation theory, and it agrees with the standard asymptotically free coupling constant of the 2-d $O(3)$ model. For large L, on the other hand, the coupling $\alpha(\theta, L)$ is θ-dependent and can only be computed non-perturbatively. The corresponding β-function is given by $\beta(\theta, \alpha) = -L\partial_L \alpha(\theta, L)$. Thanks to an ingenious use of the thermodynamic Bethe ansatz the finite-volume massgap is known analytically, both at $\theta = 0$ [32] and at $\theta = \pi$ [33]. Although the 2-d $O(3)$ model is not integrable for other values of θ, by expanding around $\theta = \pi$ some interesting analytic results have been obtained even in that regime [29]. Due to the non-vanishing massgap M at $\theta = 0$, for large L the coupling $\alpha(0, L) \to ML$ increases linearly with the volume. At $\theta = \pi$, on the other hand, the massgap vanishes and the coupling approaches a fixed point $\alpha(\pi, L) \to \alpha^\star = \pi$ as one increases $L \to \infty$. In addition to the Gaussian fixed point at $\alpha = 0$, the β-function has another zero at $\alpha^\star = \pi$, i.e. $\beta(\theta = \pi, \alpha = \pi) = 0$ [36]. Since the physics is symmetric around $\theta = \pi$, at the fixed point the β-function just touches, but does not cross zero. The double zero of the β-function thus corresponds to the lower edge of the conformal window. The parabolic form of the β-function near this fixed point causes large logarithmic finite-size corrections:

$$\beta(\alpha) \approx -C(\alpha - \alpha^\star)^2 \ \Rightarrow \ \alpha(L) \approx \alpha^\star - \frac{1}{C \log(L/L_0)} \quad (6)$$

These logarithmic corrections lead to a very slow approach to the conformal fixed point. In our model, they are associated with a marginally irrelevant operator that breaks the $O(4)$ symmetry down to $O(3)$ [34–37].

Besides the running or walking coupling, the θ-dependence of the infinite-volume massgap is also of interest. Near the fixed point at $\theta = \pi$ it is given by [36]

$$m(\theta, L \to \infty) \sim |\theta - \pi|^{2/3} |\log(|\theta - \pi|)|^{-1/2}. \quad (7)$$

The determination of $m(\theta, L)$ and $\alpha(\theta, L)$ requires non-perturbative calculations. These can be performed from first principles using lattice field theory. Simulating the 2-d lattice $O(3)$ model at large θ is very challenging due to a severe sign problem. Fortunately, the meron-cluster algorithm [38], which is based on the Wolff cluster algorithm [39], substantially reduces the sign problem and thus makes a numerical study feasible. For technical reasons related to the meron-cluster algorithm, we consider the 2-d $O(3)$ model on a triangular lattice of spatial extent L and Euclidean time extent $\beta > L$ as illustrated in Figure 1. The action is defined on nearest-neighbor bonds $\langle xy \rangle$, and is given by

$$S[\vec{e}] = \sum_{\langle xy \rangle} s(\vec{e}_x, \vec{e}_y), \quad s(\vec{e}_x, \vec{e}_y) = \frac{1}{g^2}(1 - \vec{e}_x \cdot \vec{e}_y), \quad (8)$$

for $\vec{e}_x \cdot \vec{e}_y > -\frac{1}{2}$ and $s(\vec{e}_x, \vec{e}_y) = \infty$ otherwise. This action eliminates field configurations for which the angle between neighboring spins exceeds 120 degrees, which is essential for the success of the meron-cluster algorithm. The geometric topological charge density $q_{\langle xyz\rangle} \in [-\frac{1}{2}, \frac{1}{2}]$ [40] associated with a triangle $\langle xyz\rangle$ is given by

$$R\exp(2\pi i q_{\langle xyz\rangle}) = 1 + \vec{e}_x\cdot\vec{e}_y + \vec{e}_y\cdot\vec{e}_z + \vec{e}_z\cdot\vec{e}_x + i\vec{e}_x\cdot(\vec{e}_y\times\vec{e}_z), \quad R \geq 0. \tag{9}$$

Here $4\pi q_{\langle xyz\rangle}$ is the oriented area of the spherical triangle on S^2 defined by the three unit-vectors $\vec{e}_x$, $\vec{e}_y$, and $\vec{e}_z$. By construction, the geometric lattice topological charge $Q[\vec{e}] = \sum_{\langle xyz\rangle} q_{\langle xyz\rangle}$ is an integer. In order to determine the massgap, we consider the operator $\vec{E}(t) = \sum_{x_1} \vec{e}_x$, where the sum extends over all points $x = (x_1, t)$ in a time-slice, and we define the 2-point function

$$C(t_1, t_2; \theta) = \frac{1}{Z(\theta)} \prod_x \int_{S^2} d\vec{e}_x \ \vec{E}(t_1)\cdot\vec{E}(t_2)$$
$$\times \exp(-S[\vec{e}] + i\theta Q[\vec{e}]) \sim \exp(-m(\theta, L)(t_2 - t_1)),$$
$$Z(\theta) = \prod_x \int_{S^2} d\vec{e}_x \ \exp(-S[\vec{e}] + i\theta Q[\vec{e}]), \tag{10}$$

which decays exponentially with the θ- and L-dependent massgap $m(\theta, L)$ at large Euclidean time separations.

Like in the Wolff cluster algorithm, in the meron-cluster algorithm one first chooses a reflection plane perpendicular to a randomly selected unit-vector $\vec{r} \in S^2$. In a given update step, the spins $\vec{e}_x$ are either left unchanged, or they are reflected to $\vec{e}\,'_x = \vec{e}_x - 2(\vec{e}_x\cdot\vec{r})\vec{r}$. Spins belonging to a common cluster are reflected collectively [39]. In the meron-cluster algorithm, each cluster $\mathcal{C}$ contributes an integer or half-integer to the total topological charge Q. Thanks to the 120 degrees angle constraint, the cluster topological charge $Q_{\mathcal{C}}$ is well-defined and does not depend on whether other clusters are flipped or not. Clusters with a half-integer topological charge are called meron-clusters, because they represent half-instantons. Flipping a meron-cluster changes the topological charge by an odd integer. At $\theta = \pi$ where $\exp(i\theta Q) = (-1)^Q$, this implies an exact cancellation between two contributions to the partition function. Taking this cancellation into account analytically rather than statistically via Monte Carlo leads to an improved estimator that exponentially reduces the sign problem. In a multi-cluster algorithm, for general values of θ an improved estimator for the partition function is given by

$$\frac{Z(\theta)}{Z(0)} = \langle \prod_{\mathcal{C}} \cos(\theta Q_{\mathcal{C}})\rangle. \tag{11}$$

Similarly, for the 2-point function one obtains

$$\langle \vec{e}_x\cdot\vec{e}_y \exp(i\theta Q)\rangle = \langle (\vec{e}_x\cdot\vec{r})(\vec{e}_y\cdot\vec{r}) \prod_{\mathcal{C}} \cos(\theta Q_{\mathcal{C}})$$
$$\times \left[\delta_{\mathcal{C}_x,\mathcal{C}_y} + (1-\delta_{\mathcal{C}_x,\mathcal{C}_y})\tan(\theta Q_{\mathcal{C}_x})\tan(\theta Q_{\mathcal{C}_y})\right]\rangle, \tag{12}$$

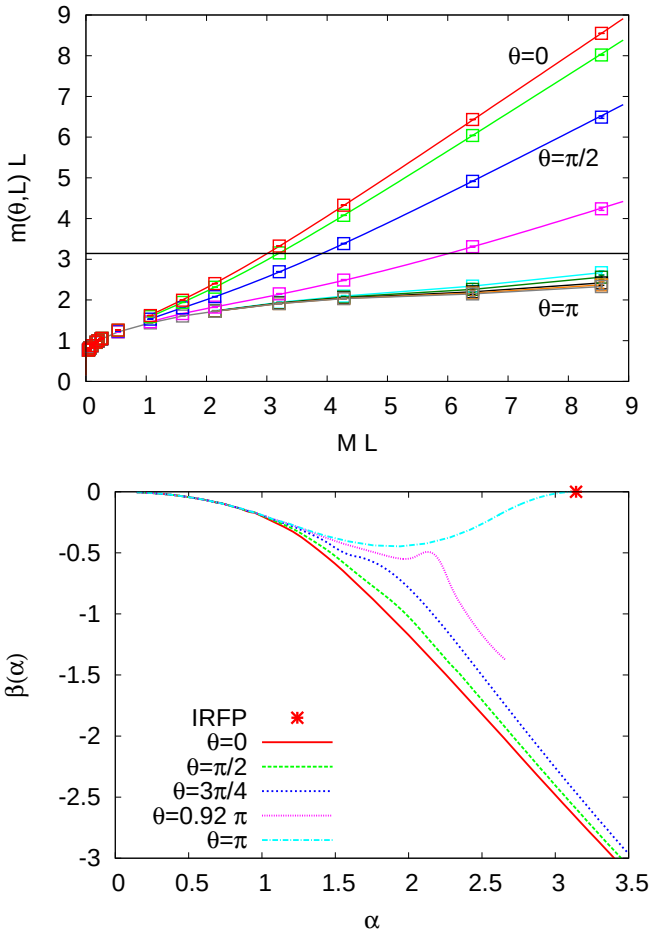

FIG. 2. *(top) The running coupling constant* $\alpha(\theta, L) = m(\theta, L)L$ *as a function of the scale set by the spatial size* L *for* $\theta/\pi = 0, 0.25, 0.50, 0.75, 0.92, 0.94, 0.96, 0.98$ *and* 1*. At* $\theta \neq \pi$ *the coupling increases linearly as* $L \to \infty$*, while at* $\theta = \pi$ *it approaches the fixed point value* π *(indicated by the horizontal line). At* $\theta \approx \pi$ *the coupling is slowly walking near the conformal fixed point. The curves for* $0 \leq \theta \leq 3\pi/4$ *show the effect of leading finite-size corrections* $\exp(-mL)/\sqrt{mL}$ *to the infinite-size massgap* m*. (bottom) The corresponding* β*-function obtained by differentiation of our numerical results, supplemented by exact values at* $\theta = \pi$ *from [33].*

where the cluster $\mathcal{C}_x$ contains x and $\mathcal{C}_y$ contains y.

We have used the meron-cluster algorithm to determine the massgap $m(\theta, L)$ for a large variety of θ-values and volumes L ranging from 6 to 100. By using at least four values of the bare coupling g, all results have been reliably extrapolated to the continuum limit. The corresponding results for the running coupling $\alpha(\theta, L)$ are illustrated at the top of Figure 2. Within error bars, they agree with values obtained from the exact massgap both at $\theta = 0$ and at $\theta = \pi$ [33]. While $\alpha(\theta, L)$ increases linearly for large L when $\theta \neq \pi$, it flattens off for $\theta = \pi$. As anticipated, due to large logarithmic corrections the approach to the fixed point is very slow. For

$\theta \approx \pi$, the coupling walks almost as slowly as at $\theta = \pi$ up to some distance scale, at which it starts running off into the linearly rising regime. While in a lattice context it is most natural to use a step scaling function [31], here we prefer to discuss the β-function that is familiar from the continuum, although its computation requires a spline-interpolation of the lattice data. The walking versus running of the coupling manifests itself in the β-function shown at the bottom of Figure 2. For $\theta \approx \pi$ it walks towards the fixed point $\beta(\theta = \pi, \alpha = \pi) = 0$ before running off (linearly) to negative values.

Figure 3 shows the finite-size scaling behavior of $m(\theta, L)L + [\pi - m(\pi, L)L]$ as a function of $MLt^{2/3}/\sqrt{|\log(t/t_0)|}$, where t is the reduced coupling $t = 1 - \theta/\pi$, and $t_0 = 70$. Large logarithmic corrections are removed in this difference between the finite-volume massgaps, so that the $L \to \infty$ value π is enforced at the critical coupling $t = 0$. The fact that all data fall on a universal curve confirms the behavior of the massgap eq.(7), and in particular the critical exponent 2/3 of the WZNW model.

It is interesting to compare the behavior of the 2-d $O(3)$ model near the conformal fixed point at $\theta = \pi$ with the anticipated behavior of walking 4-d non-Abelian technicolor gauge theories near the conformal window [25]. Both theories are asymptotically free and conformality is thus limited to scales far below $\Lambda_{\overline{MS}}$. (i) First of all, in the 2-d $O(3)$ model the parameter that determines the distance to the conformal fixed point is the continuously varying vacuum angle θ, which does not get renormalized [24, 25], and which does not affect the β-function in the perturbative regime. In walking technicolor theories, on the other hand, the corresponding parameter is the discrete number of techniquark flavors or the size of the technifermion representation, which do affect the perturbative β-function. Unlike in the 2-d $O(3)$ model, due to renormalization, one can then not directly compare physical quantities between theories in and outside the conformal window. (ii) While large, logarithmic finite-size effects are a characteristic of walking theories near the edge of the conformal window, as shown by eq.(6), their origin may differ. As we have seen, in the 2-d $O(3)$ model a marginally irrelevant operator breaks the enhanced $O(4)$ symmetry in the low-energy sector. In a 4-d non-Abelian technicolor gauge theory, it is not clear whether logarithmic corrections could come from a similar symmetry enhancement, or from conformal symmetry itself. (iii) In the 2-d $O(3)$ model the $O(4)$ symmetry enhancement causes an $O(3)$ singlet to become light as $\theta \to \pi$, in addition to the $O(3)$ triplet, all having masses much below $\Lambda_{\overline{MS}}$, before both objects become massless "unparticles" [41] at $\theta = \pi$. It has been argued that particles with a mass much below $\Lambda_{\overline{MS}}$ should also arise in walking technicolor theories near the edge of the conformal window [42, 43]. These so-called technidilatons have been identified with pseudo-Nambu-Goldstone bosons of a spontaneously broken conformal invariance, which is still weakly explicitly broken by the scale anomaly at $\Lambda_{\overline{MS}}$. In the 2-d $O(3)$ model, due to the Mermin-Wagner theorem, conformal invariance cannot break spontaneously and thus the light $O(3)$ triplet and singlet are not expected to be pseudo-Nambu-Goldstone bosons. In particular, they are exactly massless at $\theta = \pi$, despite the fact that conformal symmetry exists only in the low-energy sector and is explicitly broken at the scale $\Lambda_{\overline{MS}}$. (iv) In addition to the large finite-size effects, cut-off effects due to a finite lattice spacing a may also be important. In the 2-d $O(3)$ model, large logarithmic corrections to the expected $\mathcal{O}(a^2)$ effects mimic $\mathcal{O}(a)$ behavior [44]. Similarly, in lattice investigations of technicolor gauge theories, one must control these cut-off effects. When one uses Wilson fermions, which are theoretically cleaner than staggered fermions, without Symanzik improvement lattice artifacts are of order a. (v) Finally, in a non-Abelian gauge theory the Schrödinger functional [45] provides a definition of a running or walking coupling constant, which naturally replaces the coupling based on the finite-volume massgap that we use in the 2-d $O(3)$ model.

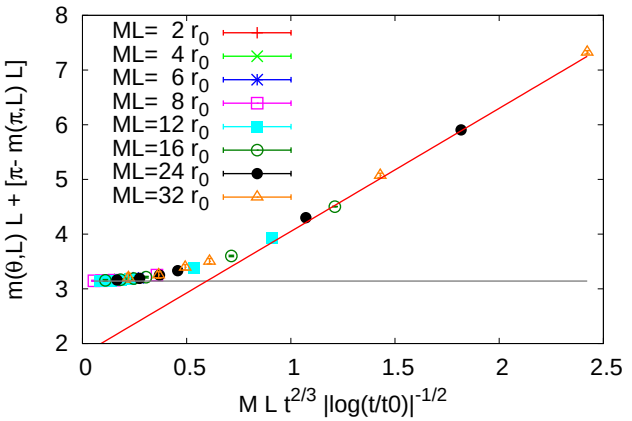

FIG. 3. *Finite-size scaling of $m(\theta, L)L$ near $\theta = \pi$ as a function of $MLt^{2/3}/\sqrt{|\log(t/t_0)|}$, with $t = 1 - \theta/\pi, t_0 = 70$. System sizes L have been chosen as multiples of r_0/M, with $r_0 = 0.26715356$ [44]. The data have been shifted by $[\pi - m(\pi, L)L]$, to eliminate the large logarithmic corrections and enforce $m(\theta = \pi, L)L = \pi$. They fall on a universal curve, confirming the critical exponent 2/3 of the WZNW model in eq.(7). This curve shows both the slow walking near π, and the linearly rising regime as $L \to \infty$.*

In the end, our study of the 2-d $O(3)$ model near $\theta = \pi$ demonstrates that slow walking can indeed be studied accurately using Monte Carlo simulations, provided that lattice artifacts and finite-volume effects, which may both be large, are well understood and under good numerical control. Besides technicolor gauge theories, it would be interesting to also investigate other models, e.g. 4-d Yang-Mills theories at non-zero θ, in order to further in-

vestigate the neighborhood of conformal fixed points.

We are indebted to J. Balog, M. Blau, C. Destri, and E. Vicari for illuminating discussions. P. de F. thanks YITP, Kyoto, for its hospitality, and M. P. acknowledges P. Ramieri for technical support. This work has been supported by the Regione Lombardia and CILEA Consortium through a LISA 2011 grant, as well as by the Schweizerischer Nationalfonds (SNF).

[1] C. Hill and E. Simmons, Phys. Rep. 381 (2003) 235.
[2] S. Weinberg, Phys. Rev. D13 (1976) 974.
[3] L. Susskind, Phys. Rev. D20 (1979) 2619.
[4] E. Farhi and L. Susskind, Phys. Rev. D20 (1979) 3404.
[5] M. E. Peskin and T. Takeuchi, Phys. Rev. Lett. 65 (1990) 964.
[6] B. Holdom, Phys. Rev. D24 (1981) 1441.
[7] T. Appelquist and L. C. R. Wijewardhana, Phys. Rev. D35 (1987) 774.
[8] D. D. Dietrich, F. Sannino, and K. Tuominen, Phys. Rev. D72 (2005) 055001.
[9] T. Banks and A. Zaks, Nucl. Phys. B196 (1982) 189.
[10] H. Gies and J. Jäckel, Eur. Phys. J. C46 (2006) 433.
[11] D. B. Kaplan, J.-W. Lee, D. T. Son, and M. A. Stephanov, Phys. Rev. D80 (2009) 125005.
[12] T. Appelquist, G. T. Fleming, and E. T. Neil, Phys. Rev. Lett. 100 (2008) 171607.
[13] A. Deuzeman, M. P. Lombardo, and E. Pallante, Phys. Lett. B670 (2008) 41.
[14] A. J. Hietanen, K. Rummukainen, and K. Tuominen, Phys. Rev. D80 (2009) 094504.
[15] Z. Fodor, K. Holland, J. Kuti, D. Nogradi, and C. Schröder, JHEP 0911 (2009) 103.
[16] L. Del Debbio, B. Lucini, A. Patella, C. Pica, and A. Rago, Phys. Rev. D82 (2010) 014510.
[17] T. DeGrand, Y. Shamir, and B. Svetitsky, Phys. Rev. D82 (2010) 054503.
[18] A. Hasenfratz, Phys. Rev. Lett. 108 (2012) 061601.
[19] A. B. Zamolodchikov and A. B. Zamolodchikov, Ann. Phys. 120 (1979) 253.
[20] A. Polyakov and P. B. Wiegmann, Phys. Lett. B131 (1983) 121.
[21] P. B. Wiegmann, Phys. Lett. B152 (1985) 209.
[22] A. B. Zamolodchikov and V. A. Fateev, Sov. Phys. JETP 63 (1986) 913.
[23] P. Hasenfratz, M. Maggiore, and F. Niedermayer, Phys. Lett. B245 (1990) 522.
[24] M. Bögli, M. Pepe, F. Niedermayer, and U.-J. Wiese, arxiv:1112:1873.
[25] D. Nogradi, arXiv:1202.4616.
[26] J. Wess and B. Zumino, Phys. Lett. B37 (1971) 95.
[27] S. P. Novikov, Sov. Math. Dokl. 24 (1981).
[28] E. Witten, Commun. Math. Phys. 92 (1984) 455.
[29] D. Controzzi and G. Mussardo, Phys. Rev. Lett. 92 (2004) 021601.
[30] M. Lüscher, Phys. Lett. B118 (1982) 391.
[31] M. Lüscher, P. Weisz, and U. Wolff, Nucl. Phys. B359 (1991) 221.
[32] J. Balog and A. Hegedus, J. Phys. A37 (2004) 1881; Nucl. Phys. B725 (2005) 531; Nucl. Phys. B829 (2010) 425.
[33] J. Balog, private communication.
[34] J. Cardy, J. Phys. A19 (1986) L1093.
[35] I. Affleck and F. D. M. Haldane, Phys. Rev. B36 (1987) 5291.
[36] I. Affleck, D. Gepner, H. J. Schulz, and T. Ziman, J. Phys. A22 (1989) 511.
[37] N. Read and R. Shankar, Nucl. Phys. B336 (1990) 457.
[38] W. Bietenholz, A. Pochinsky, and U.-J. Wiese, Phys. Rev. Lett. 75 (1995) 4524.
[39] U. Wolff, Phys. Rev. Lett. 62 (1989) 361.
[40] B. Berg and M. Lüscher, Nucl. Phys. B190 (1981) 412.
[41] H. Georgi, Phys. Rev. Lett. 98 (2007) 221601.
[42] K. Yamawaki, M. Bando, and K. Matumoto, Phys. Rev. 56 (1986) 1335.
[43] M. Hashimoto and K. Yamawaki, Phys. Rev. D83 (2011) 015008.
[44] J. Balog, F. Niedermayer, and P. Weisz, Nucl. Phys. B824 (2010) 563.
[45] M. Lüscher, R. Narayanan, P. Weisz, and U. Wolff, Nucl. Phys. B384 (1992) 168.